Overview of the FTU Results

A.A. Tuccillo 1), A. Alekseyev 2), B. Angelini 1) S.V. Annibaldi 3), M.L. Apicella 1), G. Apruzzese 1), J. Berrino 4), E. Barbato 1), A. Bertocchi 1), A. Biancalani 5), W. Bin 4), A. Botrugno 1), G. Bracco 1), S. Briguglio 1), A. Bruschi 4), P. Buratti 1) G. Calabrò 1), A. Cardinali 1), C. Castaldo 1), C. Centioli 1), R. Cesario 1), L. Chen 6), S. Cirant 4), V. Cocilovo 1), F. Crisanti 1), R. De Angelis 1), U. de Angelis 7), L. Di Matteo 1), C. Di Troia 1), B. Esposito 1), G. Fogaccia 1), D. Frigione 1), L. Gabellieri 1), F. Gandini 3), E. Giovannozzi 1), G. Granucci 4), F. Gravanti 1), G. Grossetti 4), G. Grosso 4), F. Iannone 1), H. Kroegler 1), V. Lazarev 2), E. Lazzaro 4), I.E. Lyublinski 8), G. Maddaluno 1), M. Marinucci 1), D. Marocco 1), J.R. Martin-Solis 9), G. Mazzitelli 1), C. Mazzotta 1), V. Mellera 4), F. Mirizzi 1), S. Mirnov 2), G. Monari 1), A. Moro 4), V. Muzzini 4), S. Nowak 4), F.P. Orsitto 1), L. Panaccione 1), D. Pacella 1), M. Panella 1), F. Pegoraro 5), V. Pericoli-Ridolfini 1), S. Podda 1), S. Ratynskaia 3), G. Ravera 1), A. Romano 1), A. Rufoloni 1), A. Simonetto 4), P. Smeulders 1), C. Sozzi 4), E. Sternini 1), B. Tilia 1), O. Tudisco 1), A. Vertkov 8), V. Vitale 1), G. Vlad 1), R. Zagórski 10), M. Zerbini 1), F. Zonca 1)

1) Associazione Euratom-ENEA sulla Fusione, Via E. Fermi 45, 00044 Frascati, Roma, Italy
2) TRINITI, Troitsk, Moscow Reg., Russia
3) Association Euratom-VR, Royal Institute of Technology, SE-10044 Stockholm, Sweden
4) Associazione EURATOM-ENEA, IFP-CNR, Via R. Cozzi, 53 - 20125 Milano, Italy
5) Physics Department, University of Pisa, 56127 Pisa, Italy
6) Dept. Of Physics and Astronomy, Univ. of California, Irvine, CA 92697-4575, USA and Inst. for Fusion Theory and Simulation, Zhejiang University, Hangzhou, PRC
7) Dipartimento di Fisica,Universita di Napoli and INFN Sezione di Napoli, Italy
8) FSUE “Red Star”, Electrolitnij Proezd, 1a, Moscow, 115230, Russian Federation
9) Departamento de Fısica, Universidad Carlos III De Madrid, 28911 Leganes, Madrid, Spain
10) Inst. of Plasma Physics and Laser Microfusion, EURATOM Association, 01-497, Warsaw, PL

e-mail contact of main author: tuccillo@frascati.enea.it

Abstract. Spontaneous increases of plasma density, up to ~1.6 times the Greenwald value, are observed in FTU with lithized walls. These plasmas are characterised by profile peaking up to the highest obtained densities. The transport analysis of these discharges shows a 20% enhancement of the energy confinement time, with respect to the ITER97 L-mode scaling, correlated with a threshold in the peaking factor. It has been found that 0.4 MW of ECRH power, coupled at q=2 surface, are sufficient to avoid disruptions in 0.5 MA discharges. Direct heating of magnetic islands produced by MHD modes determines current quench delay or avoidance. Supra-thermal electrons generated by 0.5 MW of Lower Hybrid power are sufficient to trigger precursors of the electron-fishbone instability. Evidence of spatial redistribution of fast electrons, on the ~100μs typical mode time scale is shown by the Fast Electrons Bremsstrahlung diagnostic. From the presence of new magnetic-island induced accumulation points in the continuous spectrum of Shear Alfvén Wave spectrum, the existence of new magnetic-island induced Alfvén Eigenmodes (MiAE) is suggested. Due to the frequency dependence on the magnetic island size, the feasibility of utilising MiAE continuum effects as novel magnetic island diagnostic is also discussed. Langmuir probes have been used on FTU to identify hypervelocity (10 km/s), micrometer size, dust grains. The Thomson scattering diagnostic was also used to characterize the dust grains, present in the FTU vacuum chamber, following a disruption. Analysis of the broad emitted light spectrum was carried out and a model taking into account the particle vaporization is compared with the data. A new oblique ECE diagnostic has been installed and the first results, both in presence of Lower Hybrid or Electron Cyclotron waves, are being compared with code predictions. A time-of-flight refractometer at 60 GHz, which could be a good candidate for the ITER density feedback control system, has been also tested.

1. Introduction

Since last FEC, FTU [1] has continued its experimental programme in support of ITER physics providing plasma scenarios and operations at ITER-relevant density and magnetic field as well as exploiting liquid lithium as plasma facing material. Moreover the combination of FTU heating systems, Electron Cyclotron Resonant Heating (ECRH, 140 GHz) and Lower Hybrid (LH, 8 GHz) [1], provides plasma scenarios with direct electron heating and current drive without momentum input as expected in ITER. In shaping the FTU scientific programme of the last two years, the emphasis has been put on emerging research themes like electron-fishbone (EFs) [2, 3], that allows addressing aspects of burning plasma non linear dynamics already in the present day machines, and on optimising operations with the Liquid Lithium Limiter (LLL) to demonstrate its capability as Plasma Facing Component (PFC) under harsh conditions [4]. Disruption avoidance has been obtained through off-axis deposition of ECRH triggered just before the quench of induced plasma disruptions. A detailed calculation of the ECRH power deposition has allowed a better understanding of the MHD behaviour, ultimately responsible for the disruption [5], and provided preliminary information on the power threshold for disruption avoidance. A strong synergy on this activity is coming from the collaboration between IPP and CRPP laboratories, allowing the comparison of similar stabilising schemes in very different plasma configurations. The well-established collaboration between FTU group, University of Pisa and University of California at Irvine has continued on the study of shear Alfvén waves (SAW) nonlinear behaviours, involving close connection and synergy between theory and experiments. Here, new structures in the low-frequency SAW continuous spectrum have been shown to exist, due to finite size magnetic islands, and the existence of new magnetic-island induced Alfvén Eigenmodes (MiAE) is suggested, when radially localized bound stated are excited within these structures. Preliminary analyses of FTU observations of Beta induced Alfvén Eigenmodes (BAE) in the presence of finite size magnetic islands [6,7,8] show BAE frequency dependences on the island width, which are consistent with the theoretical scaling of the MiAE continuum accumulation point [9]. Last but not least, some experimental time has been devoted to studying the formation and dynamics of metallic dust. In fact, hypervelocity (10 km/s), micrometer size, dust grains have been detected. Characterisation of the grains has been attempted by means of Thomson scattering diagnostic [10], analysing the light scattered by the grains produced after disruptions. Other relevant themes of the FTU programme, as the study of advanced tokamak scenarios, have been put at lower priority due to the ongoing refurbishment of heating systems. With full LH and ECRH power, advanced tokamak scenarios will be addressed again at higher current and density, thus in conditions of efficient electron-ion coupling. In this paper, results of the last two years will be overviewed: the study of high density discharges obtained with LLL will be reported in the next section, while section 3 focuses on experimental and theoretical studies of EF and SAW. Section 4 provides highlights of the results on disruption mitigation with ECRH, while section 5 summarizes those on dust. Finally, in section 6 some preliminary results on minor diagnostics upgrade will be reported, together with the planning of the near future activity on FTU.

2. Improved Performance in High Density Discharges with Lithized Walls

In a reactor relevant environment, where heat loads can exceed 20 MW/m^2, it would be of great advantage to use a liquid plasma-limiting material. This could flow in an adequate structure, thus compensating for the erosion losses due to evaporation, splashing and ion sputtering, provided that the containing structure would effectively contain the liquid under harsh conditions it should withstand.

Since 2005, a Liquid Lithium Limiter (LLL) [11] based on the Capillary Porous System (CPS) [12] has been installed on FTU.
It is located in the bottom part of the vacuum chamber, resting in the shadow of the inner side toroidal limiter. When required by the programme it can be moved and act as an effective plasma facing limiter. The LLL experiment on FTU aims at studying plasma performance in presence of lithized walls as well as at testing the CPS capability to contain liquid lithium in presence of the heavy heat loads produced in FTU. Since its installation, FTU operations have benefit of faster restarts after shutdowns, easy access to high density, up to 1.6 times the Greenwald's limit and clean operations with $Z_{Eff} \sim 1$ in a wide range of densities [13]. Interestingly, strongly peaked density profiles are obtained up to the highest density values, resembling, for many aspects, those obtained in pellet-fuelled discharges [4]. In lithized discharges, intrinsic metallic impurities (Mo, Fe, Ni) are strongly reduced ($Z_{Eff} \sim 1$), while an increase of the SOL temperature, with respect to that measured in ordinary not-lithized ohmic discharges is measured by the Langmuir probes, both at $I_P = 0.5$MA and $I_P = 0.75$MA [14]. A large database of ohmic discharges, obtained with the new LLL facility, demonstrates peculiar aspects of enhanced confinement behaviour. A detailed transport analysis of the new scenario has been performed: focusing in particular on the comparison with results of analogous studies on the bulk of ohmic "pre-lithium" FTU discharges [15].

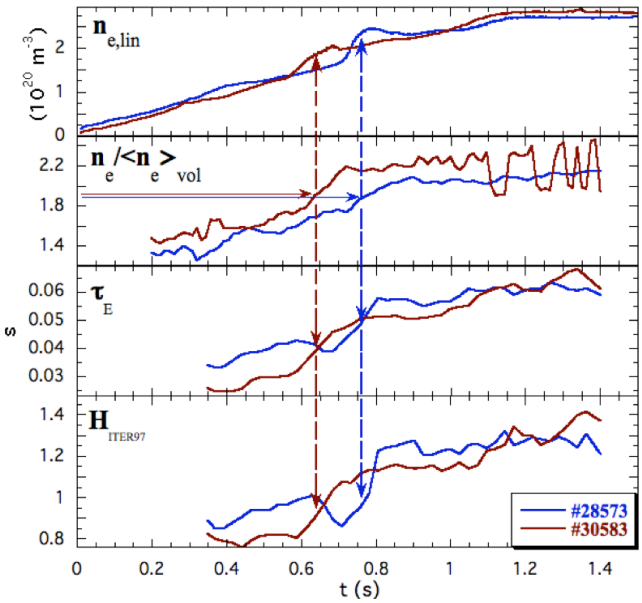

FIG 2.1 - Time evolution of line averaged density, peaking factor, energy confinement time and H_{97} in two high-density discharges. In both cases, the transition to higher τ_E occurs at the same value of $n_{e0}/\langle n_e \rangle_{vol}$.

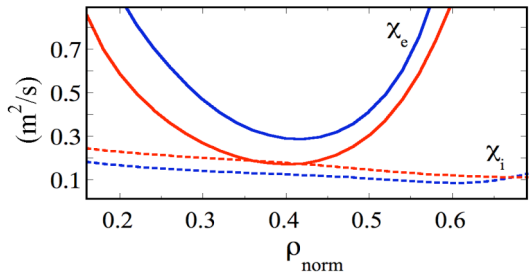

FIG 2.2 - Electron (solid lines) and ion (dashed lines) thermal conductivity for shot #28573 before (blue lines) and after (red lines) the increase of the volume density peaking factor.

The analysed database contains discharges with: $\bar{n}_e = 0.6\text{-}2.8 \times 10^{20}$ m^{-3}, $I_P = 0.5$ MA, $B_T = 6$ T, and few discharges at higher plasma current (0.7-0.75 MA). Transport analyses have been performed with the JETTO code [16], taking as input the Z_{eff} evolution from visible bremsstrahlung signals and the electron temperature and density profiles, as they respectively result from Thomson scattering and CO_2 interferometer diagnostics. The ion temperature profile is derived by assuming a neoclassical transport model with an "anomalous" multiplicative coefficient calibrated by the constraint of matching the experimental neutron rate. The radiation power density profile has been deduced from bolometry taking into account the data obtained by spectroscopy on impurities concentrations, mainly consisting of lithium and a small fraction of oxygen. In all the analyzed discharges, ion transport is neoclassical with an anomaly coefficient close to 1. As it can be seen in FIG. 2.1, where the time evolution of two high (and peaked profile) density discharges ($\bar{n}_e = 2.7 \div 2.8 \times 10^{20}$ m^{-3}) is shown, a sharp transition from a low to a higher energy confinement regime occurs around 0.6 and 0.8 s. In both discharges, the transition

seems to occur as soon as the density profile begins effectively to peak at the same threshold value of 1.75÷1.8. The improved confinement results in an enhancement of the ITER-97 L-mode scaling (H_{97}), which rises from $H_{97} \cong 0.92$ to $H_{97} \cong 1.25$.

The electron and ion thermal conductivities (χ_e and χ_i) are shown in FIG. 2.2 before and after the transition to the enhanced confinement phase. In the peaked, high-density phase, χ_e is about a factor 2 lower than in the not-peaked phase and it takes the value of ~0.2 m^2/s, which is typical of the saturated ohmic confinement (SOC) regime [15]. However, in the peaked density phase heat transport keeps being dominated by electron conductivity, while ion conductivity remains close to its neoclassical value. From the analysing the whole database of lithized discharges, the existence of the density peaking factor threshold, at which the improved confinement regime appears, seems confirmed. The results of this analysis are reported in FIG. 2.3, where the energy confinement time τ_E and the enhancement on the ITER97-L scaling H_{97} are shown versus the volume density peaking factor ($n_{e0}/\langle n_e \rangle$). The presence of a second regime of better confinement, up to a factor 1.4 above $\tau_{ITER97\text{-}L}$, come out clearly as a general behaviour of the lithized discharges, at least at $I_p = 0.5$ MA. The few analysed cases at 0.7 and 0.75 MA are also reported in the figure, but more data are needed to conclude whether an analogous transition also occurs at higher currents. It is important to note that, regardless of the density value, almost all the lithized-wall discharges tend to have peaked density profiles above the threshold value [17]. Analyses of turbulence behaviour and stability properties are in progress to assess the origin of the transition above the density peaking threshold.

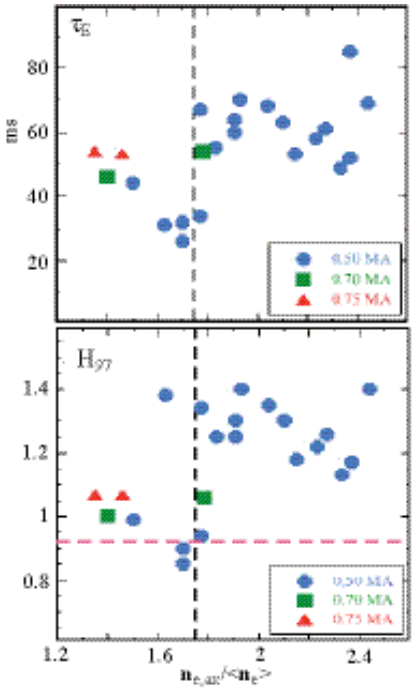

FIG 2.3 - τ_E (Top) and H_{97} (Bottom) vs. volume density peaking factor in "lithized" discharges

A statistical comparison between τ_E of the "lithized" discharges with that of the "pre-lithium" FTU ohmic discharges in the SOC phase, both gas-fuelled and pellet-fuelled, shows that the presence of lithized walls produces a rise of the saturated confinement threshold value from about 45÷50 ms to about 65÷70 ms. As in the case of pellet fuelled discharges, discussed in Refs. [5, 17], this behaviour is accompanied by a sharp increase in the peaking of the density profile and by neoclassical ion transport.

3. Theory and Modelling of Experimental Observations

Electron-fishbones in FTU plasmas. The interaction of trapped alpha particles with low frequency MHD modes in burning plasmas is characterised by small $\rho_* = \rho_L/a$, i.e. the ratio of particle Larmor radius to the machine size. That trapped particle bounce-averaged dynamics depends on energy and not on mass, together with the small ρ_*, makes trapped fusion alphas behaviour similar to that of trapped supra-thermal electron in present day experiments [2] Consequently, the fishbone-like internal kink instability driven by supra-thermal electrons generated by LHCD or ECRH and, more generally, fast electron driven MHD modes are of great interest for addressing burning plasmas issues. Fishbone-like internal kink instabilities driven by fast electrons were observed during FTU experiments aimed at producing internal transport barriers with LHCD, used to optimize the *q*-profile evolution [18].

Theoretical analyses [2] interpreted this quasi-stationary fluctuation as "fixed point" solution

of the nonlinear dynamical system, produced by supra-thermal electrons in the presence of a moderately hollow q-profile with $q_{min} \sim 1$, undergoing a transition to "limit cycle" bursting behaviour as LH power is increased. A similar instability was previously observed on DIII-D during high-field-side ECRH experiments and attributed to excitations by barely trapped supra-thermal electrons, characterised by drift reversal [19].

More recently in Tore Supra, the data of the hard-X ray diagnostic (60-80 keV) provided indication of some spatial redistribution of the suprathermal electron population [20]. However, the time behaviour of this phenomenon, with respect to the MHD time scale (0.1 ms), could not be assessed due to the insufficient time resolution of the diagnostic (16 ms). An experimental campaign has started on FTU to systematically assess the short time-scale and possibly bursting behaviour of electron-fishbones as foreseen by the theoretical model [2]. Optimal plasma conditions are provided by lithized walls [4] (low Z_{eff} and good SOL conditions for LH) and by an accurate choice of the LHCD power waveforms, which guarantees a robust control of q-profile evolution [21]. Recent experiments on FTU show that electron-fishbone activity, with "fixed point" oscillations behaviour, already appears with as low as 0.5 MW of LH power. The power is applied at the end of the ramp-up phase of an $I_P = 0.5$ MA discharge. For the duration of the LH pulse, the q-profile remains constant and is characterised by a flat central region with $q_0 \leq 1$. At the switch off of LH power, the electron-fishbone activity disappears and only sawteeth survive. Detailed analyses of MHD data provided by soft X-ray tomography [22] and of the fast electron bremsstrahlung recorded by a fast FEB camera (~4 ms overall resolution) have allowed the reconstruction of the hard x-ray emission profile on the fishbone timescale (about 0.1 ms) [3]. Preliminary results are shown in FIG. 3.1. Here, the line integrated hard x-ray profile shows a spatial redistribution of the fast electron population during typical quasi-stationary oscillations. It appears to be localised close to the radial position of mode and to occur on the same time scale. The differences between profiles are well above the error bar thanks to statistic improvements due to data integration phased with the mode oscillation [3]. The spatial redistribution seems to occur across layers centred at $r/a \approx 0.3$, with some extension to the inner and the outer half of plasma. A broadening of the hard-x ray emission is also observed comparing FEB profiles, obtained with longer integration time (3 ms), before, during and after the electron-fishbone event suggesting that an effective enhancement in transport can be ascribed to the presence of the mode.

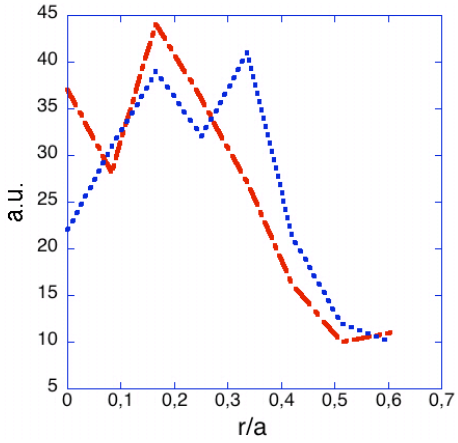

FIG 3.1 - Line integrated fast electron radial profiles by FEB camera data, obtained at different times of fishbone oscillation: during positive half period (red curve) and negative half period (blue curve). Energy range 40÷60 keV.

The effect of electron-fishbone on resonant supra-thermal electrons can be measured from FEB profiles obtained on sliding time windows with longer integration time (3 ms). From comparison of time windows centered at the beginning of the fluctuations cycle and after the peak intensity of the mode, respectively, the electorn-fisnbone induced profile broadening is seen for resonant supra-thermal electrons with energies $E \geq 40$ keV [2].

Shear Alfvén wave continuous spectrum in the presence of a magnetic island

In fusion plasmas, fast ions in the MeV energy range have velocities comparable with the typical Alfvén speed and can therefore resonantly interact with SAW. SAW in non-uniform equilibrium experience energy absorption (continuum damping [23]), due to singular

structures that are formed at the SAW continuum resonant surfaces. Because of non-uniformities along the magnetic field lines, gaps appear in the SAW continuous spectrum [24], forming regions free of continuum damping [24]. For this reason, the importance of understanding SAW continuous spectrum structure is clear when analyzing SAW stability in tokamaks and its potential impact on the fusion performance. The SAW continuous spectrum can be modified by the interaction with low-frequency MHD fluctuations, such as magnetic islands [25].

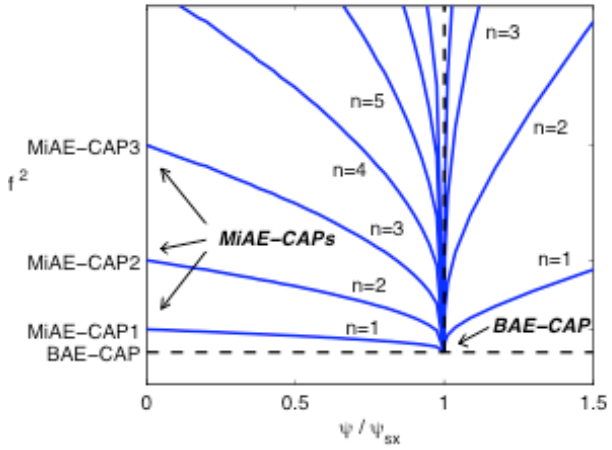

FIG 3.2 – SAW continuous spectrum for various n-modes. The BAE-CAP is shown at the separatrix (psi = psi_{sx} where psi is magnetic flux surface variable) with the new MiAE accumulation points at the O-point (psi = 0)

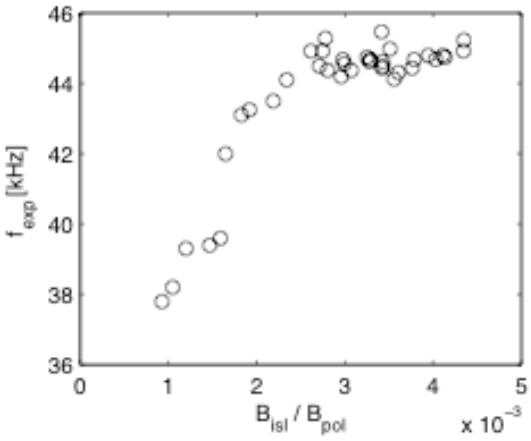

FIG 3.3 – Mode frequency versus magnetic island amplitude observed in FTU shot 25877

We derive our fluid theoretical description of the SAW continuum structure in finite-beta plasmas in presence of a finite size magnetic island [26], keeping into account geodesic curvature effects, which are responsible for the BAE gap in the low frequency SAW continuous spectrum [27]. The BAE continuum accumulation point (BAE-CAP) is shifted in space from the island rational surface, $\psi = 0$, to the separatrix flux surface position, $\psi = \psi_{sx}$, while the frequency f_{BAE} remains the same. Here, ψ is the magnetic flux coordinate. New magnetic-island induced CAPS (MiAE-CAPs) are found at the O-point of the island and, consequently, new gaps exist in the SAW continuous spectrum (see FIG. 3.2). This result has potential implications in analysis of stability properties of tokamak plasmas in presence of magnetic islands. In fact, new MiAE could be excited within a magnetic island if the thermal or energetic components of the plasma provide sufficient free energy for driving the mode. Modes in the BAE frequency range have been observed in FTU [6], in the presence of an (m, n) = (-2,-1) magnetic island, m/n indicating poloidal/toroidal mode numbers. A theoretical analysis has shown that these modes can be interpreted as BAE modes, when thermal ion transit resonances and finite ion Larmor radius effects are accounted for [7], with good agreement of measured and calculated frequencies in the small magnetic island amplitude limit. In fact, their measured frequency has been found to depend on the island amplitude as well. Similar observations have been reported by TEXTOR [8]. FIG. 3.3 shows the dependence of experimental frequency of modes seen in FTU on the magnetic island fluctuating field. This dependence is consistent with the MiAE-CAP scaling [9]. The magnetic island fluctuating field at the rational surface has been reconstructed from that at the Mirnov coil position. Due to the dependence of the MiAE-CAP frequency on mode numbers and magnetic island size, the possibility of using this scaling as novel magnetic island diagnostic is an attractive option. Information on the radial structure of the new MiAE with respect to the more conventional BAE-like gap-modes is given on the basis of mode couplings with the SAW continuum structures shown in FIG. 3.2 and their consequences on

radial mode localization. If BAEs can extend over a radial range not limited by the island size, on the contrary MiAEs are very localized and positioned at the island centre. Thus, MiAEs cannot be easily detected by diagnostic systems, which measure fluctuating fields at the plasma boundary, such as Mirnov coils. However, we could observe these modes with ECE or soft X-rays diagnostics. The fact that observed mode frequencies are lower than that of the BAE-CAP, $f_{BAE\text{-}CAP} = 60$ kHz (Te = Ti = 0.5 keV, R = 93.5 cm), confirms the interpretation of these fluctuations as BAE nonlinearly interacting with the magnetic island [7].

4. ECRH Power Acting to Control Plasma Disruptions

Control of disruptions is one of the most challenging issues for ITER operations and a key milestone to be achieved on the path to the reactor.
It can be expected, as shown in JET experiments [28], that high performance plasmas revert to L-mode regime in the pre-disruption phase, with the exception of disruptions induced by vertical displacement. Developing disruption control techniques in small experiments, with L-mode plasmas, would then be directly relevant for ITER and future reactors-grade machines. Presently "massive gas injection" seems to be the most likely candidate for disruption control in ITER, although the use of ECRH represents an excellent alternative. Recent experiments on FTU [29, 5], as well as on ASDEX Upgrade [30, 5], indicate how the application of ECRH at specific radial locations can prevent or postpone the disruption.
Disruptions are induced on FTU by injecting Mo into the plasma via laser blow-off, and only in a few cases by puffing deuterium above Greenwald limit. In the latter case the discharges are limited at 0.35 MA to avoid the 140 GHz ECRH density cut-off, $n_{e\text{-}cutoff} \sim 2.4\times10^{20}$ m^{-3}. Disruptions control is then studied by triggering ECRH power at a pre-selected loop voltage level (about twice the level in steady state the phase) with pulse duration normally of 30 ms. Magnetic field is kept constant ($B_T = 5.3$T) while the ECRH launching mirrors are steered, before every discharge, to inject the power at different plasma locations. A comparison of two discharges with and without ECRH is shown in FIG. 4.1. Typically, the modes grow up, quickly slow down and then lock. The application of ECRH modifies the starting time of the current quench according to power deposition location (r_{dep}). Disruption avoidance and complete discharge recovery is obtained when P_{ECRH} is applied on rational surfaces, whereas the current quench is progressively delayed when the r_{dep} is approaching a rational surface from the outer side.

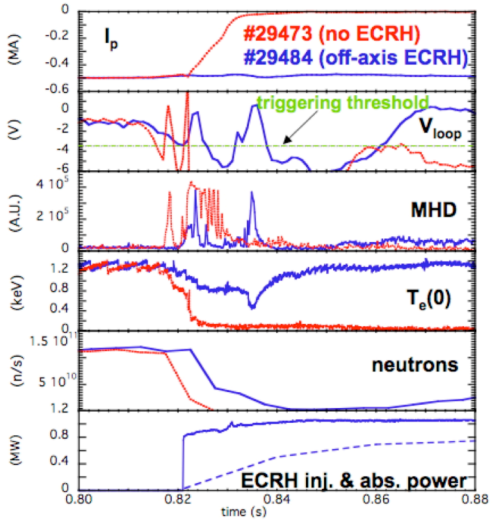

FIG 4.1 - Comparison between two FTU discharges with/without ECRH. The disruption is avoided in #29484 with ECRH injection on the q=2 surface

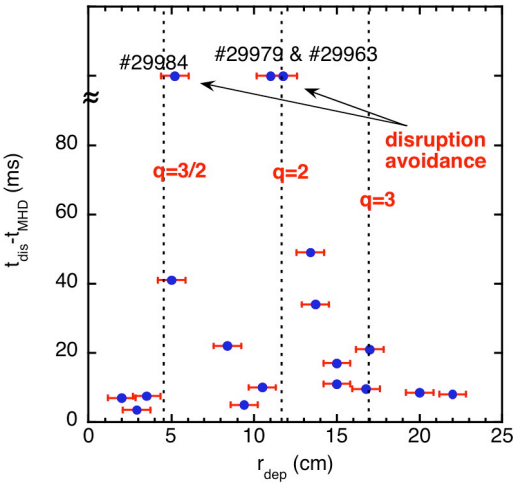

FIG 4.2 - FTU power deposition scan: current quench delay vs. r_{dep}; t_{dis} = time of current quench; t_{MHD} = time of abrupt rise of MHD activity. The vertical axis is interrupted above 80 ms to accomodate discharges with disruption avoidance.

The analysis of Mirnov coils, fast ECE and soft x-ray tomography shows that m/n=3/2, 2/1, 3/1 modes are generally present with the 2/1 having the largest amplitude. Direct heating, above a threshold value, of one of the magnetic islands prevents its further growth and produces the stabilization of the other coupled MHD modes avoiding or delaying the current quench as summarised in FIG. 4.2.

Injected P_{ECRH} has been varied in the range 0.4-1.2 MW and the absorbed fraction has been evaluated by the ECWGB 3D code [31]. An ECRH power of 0.4 MW, deposited at the q = 2 surface, is sufficient to avoid disruptions in 0.5 MA discharges while in a 0.35 MA discharge 0.8 MW are needed. The Rutherford equation [32] has been used to reproduce the evolution of the MHD modes that are found to be conventional tearing modes stabilized by a strong local ECRH heating. The results of the simulation for discharge 29479 are compared with the experimental data in FIG. 4.3.

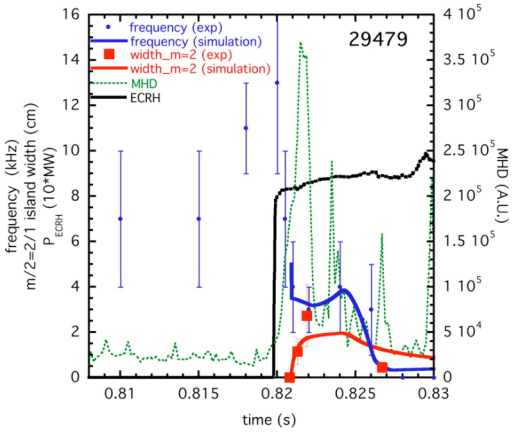

FIG 4.3 - Time evolution of 2/1mode, close to mode locking time, compared with Rutherford model. Experimental frequency from Mirnov coils, MHD represents the B_θ oscillations envelope and island width is determined from soft x-ray tomography.

The mode coupling effects resulting from the FTU r_{dep} scans are interesting in view of a possible application of such ECRH control technique to ITER. Various schemes can be envisaged in order to suppress islands that are not directly heated by ECRH waves. In density limit disruptions, when ECRH cannot be absorbed on the central 3/2 mode due the density cut-off, avoidance might be obtained by heating a more external coupled island where the density is below cut-off. In other cases, P_{ECRH} might be deposited on the coupled island that requires less power for stabilization.

5. Investigating Dust Dynamics in Tokamak Plasma

Since 2005, research activity on dust in fusion plasma has been pursued on FTU in collaboration with the Max Planck Institute for Extraterrestrial Physics (MPE) of Garching, the Royal Institute of Technology (KTH) of Stockholm and the Unversities of Naples and Molise. Theoretical issues on dusty plasma physics [33, 34] have been addressed and experiments have been performed on FTU [35, 36, 37]. The detection, in the FTU SOL, of micron size fast dust particles, impinging on plasma facing components at velocity of the order of 10 km/s, has been already reported [35]. Such particles produced uncorrelated spikes in the ion saturation current signal detected by two adjacent Langmuir probes. Interpretation of these events in terms of the dust impact ionization events was supported by the SEM observation of typical impact craters on the probe surface. A more accurate analysis [36] has shown that the impact ionization events can be identified by suitable choice of the threshold amplitude of the observed spikes. The number of the impact events detected matches reasonably the number of the craters observed. Analysis of the features of the spiky signals as well of the morphology of the craters observed, see FIG. 5.1, suggests the exclusion of possible alternative interpretations. To this end, an experimental campaign was planned to collect and analyze fast grains by silica aereogel targets [38]. This highly porous, very low density material allows capture of the fast dust particles without affecting them, and might provide information on the velocity and size distribution as well as on the dust composition. A preliminary assessment of the compatibility of silica aereogel targets with the FTU vacuum and plasma operation was carried out. The mechanical design and construction of the sample

holder has been done and the sample introduction system has been improved to allow the aereogel experiments in the next campaign. The feasibility of this new method of dust collection has been suggested by preliminary tests on the HT-7 [39] and in the reversed field pinch EXTRAP-T2R [39]. A design has been undertaken of an electro optical probe to detect the emission of light associated with a dust impact ionization event and simultaneously record the perturbation (spike) it will produce on the ion saturation current.

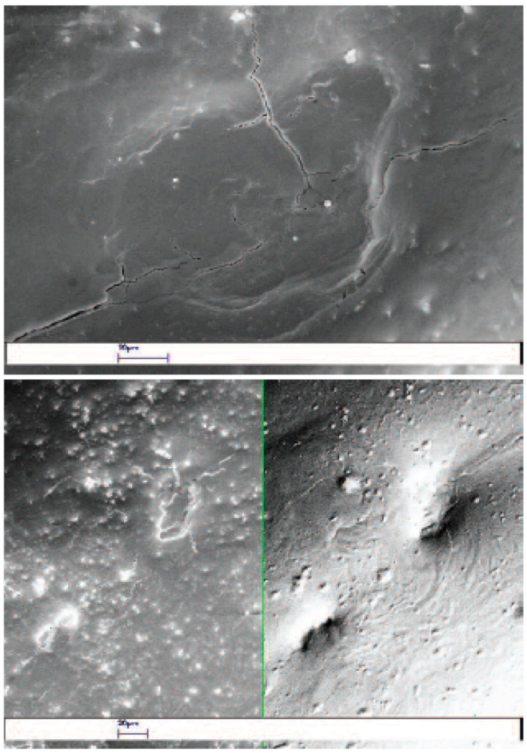

FIG 5.1 - SEM analysis of the probe surface exposed to the FTU plasma. The scales indicated are 10 μm in the upper figure, taken by secondary electron detector (SED) and 20 μm for the lower figure, where SED (left) and EBS (electron back scattering, right) images are compared for the same probe area

A characterization of the molibdenum (main limiter material in FTU) dust component present in the FTU vacuum chamber has been attempted by laser light elastic scattering [37]. The detection channels at the laser wavelength ($\lambda = 1064$ nm) of the Thomson scattering diagnostic were used. The signal was detected on many discharges after disruption. No evidence of scattering by dust was found indeed in the main plasma during normal operations, nor was possible to look at the SOL as no channels are aiming there. The particle size was estimated from the intensity of the scattered light, with Rayleigh modelling of the laser-dust elastic cross section. This approximation seems reasonable for particles with size less than 0.1 μm (about 10% λ); however, the diagnostics becomes very insensitive to particles smaller than a few tens nanometers. Assuming typical values of the refractive index expected for molybdenum dust grains, the average radius of the dust grains detected after disruption was found of the order of 50 nm. The average dust density was found about 10^7 m^{-3}, calculated as the total number of scattering events, divided by the product of the scattering volume and the total number of the laser pulses considered. The size distribution of the particles seems to follow a power law σ^{-2}, where σ is the geometrical cross section of the grains [10].

6. Minor Upgrades and Future Plans

Since last FEC a long-term programme of upgrading has been undertaken on FTU. Main objective is the refurbishment of the heating systems, to have the full power reinstated, together with the realisation of a new launching structure for ECRH. This structure will be steerable in real time, will allow a CTS experiment in an ITER relevant configuration and will allow injection at large off-normal angle. In particular this latter capability will be used to operate in mode conversion thus enabling heating high density peaked plasmas above the 140 GHz cut-off density. Minor diagnostics upgrades have been already completed and have initiated the commissioning on FTU: Oblique ECE, Refractometer and MSE. The MSE commissioing has been slowed down due to hardware rearrangement needed to optimise detection and signal to noise ratio. This has been an acceptable limitation as in parallel the experimentation on advanced scenarii has been delayed by the RF power refurbishment.

A prototype of a time-of-flight refractometer at 60 GHz, has been tested in FTU, in collaboration with TRINITI institute (Moscow). Line density measurements are in good agreement with those measured with CO_2 interferometer. This system has reduced size, does not require mirrors inside the vessel and is not affected by fringe jumps: therefore it seems to be a good candidate for the ITER density feedback control. A system with two frequencies is under development.

The antenna of the ECE Grating Polychromator (GPC) has been modified to steer its lines of sight in toroidal direction from 90° to 72°. EC Emission at different angles comes from different regions of the electron distribution function, providing a diagnostic of possible distortions of the maxwellian. The information can be reconstructed using an emission code where the distribution function is the trial function. Preliminary results have been obtained during LHCD, where a suprathermal electron tail is driven, and during a strong central ECRH at low density, where the bulk of the distribution is directly affected. During LHCD, at intermediate density (~$9x10^{19}m^{-3}$), the second harmonic X-mode emission at 77° is higher than that measured at 90° by the Michelson interferometer (see FIG. 6.1), as expected for the contribution of the upshifted emission that is not reabsorbed by the thermal electrons. The difference between the two emissions is an indication of the number of the "upshifted electrons" and their energy. The data interpretation, however, is much more complex considering that a) suprathermal emission is not radially localized, b) at higher frequencies (above 350 GHz) the third harmonic down shifted emission overlaps the second harmonic, c) the O-mode contribution is not negligible. Measurements during strong ECRH heating, in the current ramp-up, are even more difficult to reconstruct as the distortion of the distributions can only be obtained by a Fokker-Plank code. The only clear effect on the emission is a stronger decrease with the observation angle respect to that of thermal plasmas. The distortion found in previous works [40, 41] is an asymmetric flattening of the distribution function at the resonance.

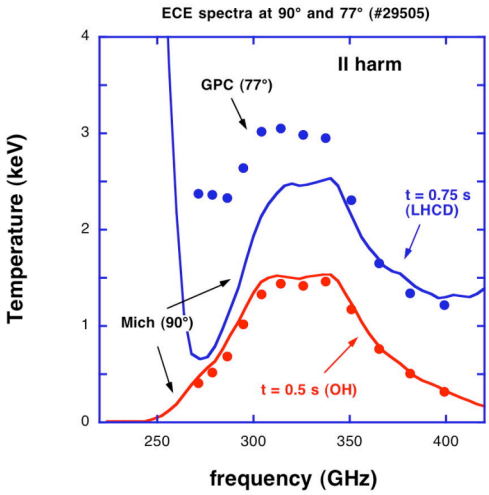

FIG 6.1 – ECE emission at 90° (lines) and 72° (dots) in OH (red) and LHCD (blue) phase

References

[1] SPECIAL ISSUE on FTU Guest editor GORMEZANO C., Fusion Sci. Techn. **45** (2004)

[2] ZONCA, F., et al., "Electron fishbones: theory and experimental evidence", Nucl. Fusion **47** (2007) 1588

[3] CESARIO, R., et al., "Fishbone-like instability driven by LH generated fast electrons on FTU", EX-P8-12 this conference

[4] MAZZITELLI, G., "Status and Perspectives of the Liquid Material Experiments in FTU and ISTTOK", EX-P4-6 et al., this conference

[5] ESPOSITO, B., et al., "Disruption Control on FTU with ECRH", EX/7-3Ra this conference

[6] BURATTI, P., et al., “Observation of high-frequency waves during strong tearing mode activity in FTU plasmas without fast ions”, Nucl. Fusion **45** (2005) 1446
[7] ANNIBALDI, S.V., et al., “Excitation of beta-induced Alfvén eigenmodes in the presence of a magnetic island”, Plasma Phys. Control. Fusion **49** (2007) 475
[8] ZIMMERMANN, O., et.al., “Coupling of Alfvén-like modes and large 2/1 tearing modes at TEXTOR” 2005 (Proc. 32nd EPS Conf. on Plasma Phys. Control. Fusion, Tarragona, 2005) ECA **29C** (2005) P-4.059
[9] BIANCALANI, A., et al., “Shear Alfvén wave continuous spectrum in the presence of a magnetic island“, TH/P3-5 this conference
[10] CASTALDO, C., et al., "Dust detection in FTU”, EX/P4-5 this conference
[11] APICELLA, M., L., et al., “First experiments with lithium limiter on FTU”, J. Nucl. Mater. 363-365 (2007) 1346
[12] EVTIKHIN, V., A., et al., “Technological aspects of lithium capillary-pore systems application in tokamak device”, *Fusion Eng. Des.* **V. 56-57** (2001) 363
[13] MAZZITELLI, G., et al., “Experiments on FTU with a liquid lithium limiter”, 34th EPS Conference on Plasma Phys. Warsaw, 2 - 6 July 2007 ECA Vol.31F, O-2.001 (2007)
[14] PERICOLI-RIDOLFINI, V., et al., “Edge properties with the liquid lithium limiter in FTU-experiment and transport modelling Plasma Phys. Control. Fusion **49** (2007) S123
[15] ESPOSITO, B., et al., “*Transport Analysis of ohmic, L-mode and improved confinement discharges in FTU”* Plasma Phys Control. Fusion. **46** (2004) 1793
[16] CENACCHI, G. and TARONI, A., "The JET Equilibrium-Transport Code for free Boundary Plasmas", in Proc. 8th Computational Physics, Computing in Plasma Physics, Eibsee 1986, (EPS 1986), Vol. 10D, 57
[17] ROMANELLI, M., et al., “Confinement and turbulence study in the Frascati Tokamak Upgrade high field and high density plasmas” Nucl. Fusion. **46** (2006) 412
[18] PERICOLI-RIDOLFINI, V., et al., “Overview of FTU Results”, Nucl. Fusion **47** (2007) S608
[19] WONG, K., L., et al., “Internal Kink Instability during Off-Axis Electron Cyclotron Current Drive in the DIII-D Tokamak”, Phys. Rev. Lett. **85** (2000) 996
[20] MACOR, A., et al., “Fast particle triggered modes: experimental investigation of Electron Fishbones on TORE SUPRA”, 35th EPS Conference on Plasma Phys. Crete, 9 - 13 June 2008 P-4.062
[21] CESARIO, R., et al., “ Modeling of Lower Hybrid Current Drive by including spectral broadening induced by Parametric Instability in Tokamak Plasmas” Phys. Rev. Lett., **92** 17 (2004) 175002
[22] SMEULDERS, P., “Tomography on Lao-Hirschman Type of Equilibria using Mode Rotation” 34th EPS Conference on Plasma Phys. Warsaw, 2 - 6 July 2007 ECA Vol.31F, P-5.069 (2007)
[23] CHEN, L., HASEGAWA, A., “Plasma heating by spatial resonance of Alfvén wave”, Phys. Fluids **17** (1974) 1399
[24] KIERAS, C.E., TATARONIS, J.A., “The shear-Alfvén continuous spectrum of axisymmetric toroidal equilibria in the large aspect ration limit”, J. Plasma Phys. **28** (1982) 395
[25] FURTH, H.P., et al., “Finite resistive instabilities of a sheet pinch”, Phys. Fluids **6** (1963) 459
[26] BIANCALANI, A., et al., “Continuous spectrum of shear Alfvén waves in the presence of a magnetic island” 35th EPS Plasma Physics Conference, 9–13 June 2008, Hersonissos, Crete, Greece (2008)

[27] CHU, M.S., et al., “A numerical study of the high-n shear Alfvén spectrum gap and the high-n gap mode”, Phys. Fluids **B 4** (1992) 3713
[28] RICCARDO, V. and LOARTE, A., "Timescale and magnitude of plasma thermal energy loss before and during disruptions in JET ", Nucl. Fusion **45** (2005) 1427
[29] ESPOSITO, B., et al., "Disruption Avoidance in the Frascati Tokamak Upgrade by Means of Magnetohydrodynamic Mode Stabilization Using Electron-Cyclotron-Resonance Heating", Phys. Rev. Lett. **100** (2008) 045006-1
[30] ZOHM, H., et al., " MHD stability and disruption physics in ASDEX Upgrade", Plasma Phys. Control. Fusion **37** (1995) A313
[31] NOWAK, S. and OREFICE, A., "Three-dimensional propagation and absorption of high frequency Gaussian beams in magnetoactive plasmas", Phys. Plasmas **1** (1994) 1242
[32] RAMPONI, G., et al., "On the stabilization of neoclassical tearing modes by electron cyclotron waves ", Phys. Plasmas **6** (1994) 3561
[33] CASTALDO, C., et al., ”Screening and attraction of dust particles in plasmas”, Phys. Rev. Lett. , **96** (2006) 075004
[34] DE ANGELIS, U., et al., “Fluctuations in dusty plasmas”, Plasma Phys. Control. Fusion, **48** (2006), B91
[35] CASTALDO, C., et al., “Diagnostic of fast dust particles in tokamak edge plasmas”, Nucl. Fusion, **47** (2007) L5
[36] RATYNSKAIA, S., et al., “Hypervelocity dust impacts in FTU scrape-off layer”, Nucl. Fusion, **48** (2008) 015006
[37] GIOVANNOZZI, E., et al., ”Dust measurement with Thomson scattering in FTU”, in “Burning Plasma Diagnostics International Conference”, Varenna, Italy 24-28 September 2007, AIP Conf. Proc. Vol. 988, pg. 148
[38] TSOU, P., “Silica aereogel captures cosmic dust intact”, J. Non-Crys. Solids, **186** (1995), 415
[39] RATYNSKAIA, S., private communication
[40] TUDISCO, O., et al, “Oblique ECE Measurements during Strong ECH at 140 GHz in FTU” 28th EPS Conf. on Contr. Fusion and Plasma Phys., Funchal 2001, **25A** 1221 p3.082
[41] KRIVENSKI, V., “Electron cyclotron emission by non-Maxwellian bulk distribution functions” 11th Joint Workshop on ECE and ECRH, Fusion Eng. Des. **53** (2001) 23